

## RESEARCH ARTICLE

# Interfacial amino acids support Spa47 oligomerization and *shigella* type three secretion system activation

Hannah J. Demler<sup>†</sup>  | Heather B. Case<sup>†</sup>  | Yalemi Morales  | Abram R. Bernard  | Sean J. Johnson  | Nicholas E. Dickenson 

Department of Chemistry and Biochemistry,  
Utah State University, Logan, Utah

**Correspondence**

Nicholas E. Dickenson, Department of  
Chemistry and Biochemistry, Utah State  
University, Logan, UT 84322.  
Email: nick.dickenson@usu.edu

**Funding information**

National Science Foundation, Grant/Award  
Number: 1530862; National Institutes of  
Health, Grant/Award Number:  
1R15AI124108-01A1

**Abstract**

Like many Gram-negative pathogens, *Shigella* rely on a type three secretion system (T3SS) for injection of effector proteins directly into eukaryotic host cells to initiate and sustain infection. Protein secretion through the needle-like type three secretion apparatus (T3SA) requires ATP hydrolysis by the T3SS ATPase Spa47, making it a likely target for in vivo regulation of T3SS activity and an attractive target for small molecule therapeutics against shigellosis. Here, we developed a model of an activated Spa47 homo-hexamer, identifying two distinct regions at each protomer interface that we hypothesized to provide intermolecular interactions supporting Spa47 oligomerization and enzymatic activation. Mutational analysis and a series of high-resolution crystal structures confirm the importance of these residues, as many of the engineered mutants are unable to form oligomers and efficiently hydrolyze ATP in vitro. Furthermore, in vivo evaluation of *Shigella* virulence phenotype uncovered a strong correlation between T3SS effector protein secretion, host cell membrane disruption, and cellular invasion by the tested mutant strains, suggesting that perturbation of the identified interfacial residues/interactions influences Spa47 activity through preventing oligomer formation, which in turn regulates *Shigella* virulence. The most impactful mutations are observed within the conserved Site 2 interface where the native residues support oligomerization and likely contribute to a complex hydrogen bonding network that organizes the active site and supports catalysis. The critical reliance on these conserved residues suggests that aspects of T3SS regulation may also be conserved, providing promise for the development of a cross-species therapeutic that broadly targets T3SS ATPase oligomerization and activation.

**KEYWORDS**

ATPase, catalysis, oligomerization, Spa47, T3SS, type 3 secretion system, virulence regulation

**Abbreviations:** AEBFSF, 4-(2-aminoethyl) benzenesulfonyl fluoride hydrochloride; BSA, bovine serum albumin; CBD, chitin binding domain; DMEM, Dulbecco's Modified Eagle Medium; DTT, dithiothreitol; EDTA, ethylenediaminetetraacetic acid; GAPDH, glyceraldehyde-3-phosphate dehydrogenase; IPTG, Isopropyl  $\beta$ -D-1-thiogalactopyranoside; LB, Luria-Bertani; LPS, lipopolysaccharide; PBS, phosphate buffered saline; PDVF, polyvinylidene fluoride; PMF, proton motive force; RMSD, root-mean-square deviation; T3SA, type three secretion apparatus; T3SS, type three secretion system; TB, terrific broth; TEM, transmission electron microscopy; TLC, thin layer chromatography; TSA, tryptic soy agar; TSB, tryptic soy broth.

<sup>†</sup>Authors contributed equally to this work.

## 1 | INTRODUCTION

*Shigella* is a genus of nonmotile, facultative anaerobic, Gram-negative bacteria belonging to the family Enterobacteriaceae. Infection by any one of the four *Shigella* species results in shigellosis, a severe form of bacillary dysentery hallmarked by colonic mucosal inflammation and bloody diarrhea. The debilitating symptoms, low infectious dose (10–100 organisms),<sup>1</sup> and rapid emergence of antibiotic and multi-antibiotic resistant strains result in an estimated 90 million annual infections and more than 100 000 deaths per year, making *Shigella* a worldwide health concern.<sup>2,3</sup> The highest mortality rate, however, is observed among children living in developing countries lacking access to clean drinking water and proper medical care.<sup>4</sup> With no FDA approved vaccine against *Shigella* yet available, it is likely that without active intervention, *Shigella* infections will continue to be one of the leading bacterial causes of diarrheal disease and a significant global health burden. These alarming factors underscore the urgent need to better understand the molecular mechanisms responsible for activation and regulation of *Shigella's* primary virulence factor, the type three secretion system (T3SS).

The T3SS is an elegant nanomachine shared by many Gram-negative bacteria, including *Shigella*, *Salmonella*, *Escherichia coli*, *Chlamydia*, *Yersinia*, and others.<sup>5–7</sup> Each of these pathogens is reliant on their T3SS(s) as a primary virulence factor that injects an arsenal of bacterial effector proteins directly into the host cell cytoplasm. While the roles of the injected effector proteins are pathogen specific and tailored to the pathogens' infective environments and replicative niches, the effectors are all secreted through a highly conserved needle-like type three secretion apparatus (T3SA) and generally support host cell infection and evasion of host immune responses.<sup>8</sup> Kubori and colleagues first visualized negative-stained structures of the T3SA via transmission electron microscopy (TEM) in 1998.<sup>9</sup> These original images and a more recent series of TEM and cryo-electron tomography 3D structures clearly show that the T3SA consists of a basal body that anchors the apparatus to the bacterial inner and outer membranes, a hollow needle-like structure that extends from the basal body past the membrane-associated lipopolysaccharide (LPS) layer, and an associated protein complex that resides at the tip of the needle and penetrates the eukaryotic host cell membrane.<sup>10–13</sup> Additionally, several of the most recent studies show that the T3SA contains a cytoplasmic protein complex associated with the apparatus basal body and that this complex includes a highly conserved homooligomeric ATPase that supports protein secretion through the apparatus.<sup>10,14</sup> We have previously demonstrated that the *Shigella* protein Spa47 is a T3SS ATPase whose activity is essential for protein secretion through the apparatus and overall *Shigella* virulence.<sup>15,16</sup> Furthermore, Spa47 oligomerization is required for ATPase activity, as residues from opposite sides of adjacent Spa47 protomers contribute to interfacial active sites within the complex, making Spa47 oligomerization a likely means of regulating T3SS activity in vivo and an attractive target for nonantibiotic therapeutics against *Shigella* infections.<sup>17</sup>

Here, we use a recently solved Spa47 crystal structure<sup>15</sup> to develop a homo-hexameric model of the activated Spa47 complex and identify interfacial residues that are involved in Spa47 oligomerization. The identified residues cluster to two independent sites at the interface between Spa47 protomers where they appear to be involved in a complex hydrogen bonding network that supports Spa47 oligomerization and catalysis. Each of the identified residues was mutated to an oppositely charged amino acid as well as to alanine in an effort to disrupt the predicted interactions. Indeed, several of the engineered mutations had a significant negative influence on oligomer formation and enzyme activity in vitro as well as T3SS activity and *Shigella* virulence phenotype in vivo. High-resolution crystal structures of ten of the Spa47 mutants verified the intended mutations and showed that the overall integrity of the protein structure was unaffected, supporting our hypothesis that the observed effects resulted from perturbed intermolecular interactions. Together, these findings begin to assemble an important molecular description of Spa47 oligomerization and the influences it has on T3SS activity and *Shigella* virulence phenotype while additionally identifying precise and highly-conserved targets for much needed anti-infective therapeutics against T3SS ATPases.

## 2 | EXPERIMENTAL PROCEDURES

### 2.1 | Materials

Wild-type *S. flexneri* corresponds to the serotype 2a 2457T strain originally isolated in 1954.<sup>18</sup> The *S. flexneri spa47* null strain was engineered by Abdelmounaaim Allaoui as described in Jouihri et al.<sup>19</sup> *E. coli* strains and 2X ligation mix were from Novagen (Madison, WI). Restriction enzymes, the pTYB21 protein expression plasmid, PCR buffer, Phusion High-Fidelity polymerase, and chitin resin were purchased from New England Biolabs (Ipswich, MA). Oligonucleotide primers and the synthesized *spa47* gene were from Integrated DNA Technologies (Coralville, IA). Defibrinated sheep blood was from Colorado Serum Company (Denver, CO), and HeLa cells were from the American Type Culture Collection (Manassas, VA). The Superdex 200 Increase size-exclusion column and 5 mL HiTrapQ resin were purchased from GE Healthcare (Pittsburgh, PA). ATP was from Sigma-Aldrich (St. Louis, MO) and  $\alpha$ -<sup>32</sup>P-ATP was from Perkin Elmer (Boston, MA). Dithiothreitol (DTT) and ampicillin were from Gold Biotechnology (St. Louis, MO). Rabbit anti-IpaC antibodies and the pWPSf4 plasmid were generous gifts from Wendy and William Picking (University of Kansas). DyLight 488 conjugated mouse anti-glyceraldehyde 3-phosphate dehydrogenase and Alexa Fluor 647 goat anti-rabbit antibodies were purchased from Thermo Scientific (Rockford, IL). All other solutions and chemicals were of reagent grade. The UniProtKB accession number for Spa47 is POA1C1.

### 2.2 | Cloning

The *spa47* gene was purchased as a double-stranded gBlock product from Integrated DNA Technologies with modifications for cloning into the expression plasmid pTYB21, which encodes an N-terminal chitin

binding domain (CBD) and intein linker as described previously.<sup>16</sup> Each of the Spa47 point mutants described in this study was generated in the expression plasmid pTYB21 using inverse PCR and the wild-type *spa47*/pTYB21 construct as a template. Wild-type *spa47* and each of the tested mutants was additionally cloned into the plasmid pWPsf4 using primers that encode 5' NdeI and 3' BamHI restriction sites. Spa47 constructs lacking the N-terminal 79 residues were generated using inverse PCR and the *spa47* mutants in pTYB21 as a template. Primer sequences are available upon request. All constructs were sequence verified by Sanger sequencing (Genewiz, Inc., South Plainfield, NJ).

### 2.3 | Protein expression and purification

Spa47 and each of the Spa47 mutants encoded in pTYB21 were transformed into *E. coli* Tuner (DE3) cells, expressed, and purified as previously described.<sup>16</sup> Briefly, the transformed *E. coli* cells were grown to an OD<sub>600</sub> of 0.8 in Terrific Broth media containing 0.1 mg/mL ampicillin at 37°C, 200 RPM. The culture was cooled to 17°C and induced with 1 mM IPTG for approximately 20 h (17°C, 200 RPM). All subsequent steps were carried out at 4°C (or on ice) unless otherwise stated. The bacteria were pelleted by centrifugation, resuspended in binding buffer (20 mM Tris, 500 mM NaCl, pH 7.9) containing 0.2 mM of the protease inhibitor 4-(2-aminoethyl) benzenesulfonyl fluoride hydrochloride (AEBSF), lysed by sonication, and purified using a chitin affinity column. The purified Spa47 protein was eluted using on-column cleavage of the intein linker domain by exposure to binding buffer containing 50 mM DTT. The elution fractions were diluted, resulting in a final buffer concentration of 20 mM Tris, 100 mM NaCl, 5 mM DTT, pH 7.9, supporting additional purification by anion exchange chromatography. Wild-type Spa47 and most of the purified mutants do not bind the anion exchange resin under these conditions, resulting in purified Spa47 in the flow through. Spa47<sup>R271E</sup> bound the anion exchange column tightly and was eluted using a 100 mM to 1 M NaCl elution gradient. The purified Spa47 was concentrated using Sartorius centrifugal filter units with a 30 kDa molecular weight cutoff and further purified/characterized using a Superdex 200 16/600 size exclusion column equilibrated with 20 mM Tris, 100 mM NaCl, 5 mM DTT, pH 7.9 followed by SDS-PAGE. Spa47 concentrations were determined using gel densitometry of Coomassie stained acrylamide gels and bovine serum albumin as a standard, as previously reported and validated.<sup>16</sup> All Spa47 concentrations are reported in monomer concentration units for consistency and clarity.

### 2.4 | Spa47 crystallization

Crystallization of engineered Spa47<sup>Δ1-79</sup> point mutation variants was performed using standard vapor diffusion methods in conditions similar to those previously identified for the wild-type Spa47<sup>Δ1-79</sup> construct.<sup>15</sup> For each construct, drops containing 3 μL protein (10–20 mg/mL) and 1 μL well solution were set up by hanging drop vapor diffusion with well conditions containing 0.1 M Tris pH 8.5, 0.2 M ammonium acetate, 0.2 M lithium sulfate, 20% - 26% PEG

4000, and 5.5% - 10.5% MPD. Small rod-like crystals were observed after approximately eight hours at room temperature (20–22°C).

### 2.5 | Crystallographic data collection and structure determination

Crystallographic data for each Spa47<sup>Δ1-79</sup> point mutation variant were collected on beamlines 9-2 and 14-1 at the Stanford Synchrotron Radiation Lightsource. Data were processed using HKL2000.<sup>20</sup> The crystals belong to space group P 21 and contain two molecules in the asymmetric unit (Matthews coefficient = 2.3, 45% solvent). The structures were solved by molecular replacement using the published wild-type Spa47<sup>Δ1-79</sup> structure (PDB ID 5SWJ) as the search model. PHENIX<sup>21</sup> was used to perform individual b-factor, positional, and TLS refinement. Final refinement statistics are shown for each structure in Supplementary Table S1.

### 2.6 | Size-exclusion chromatography evaluation of Spa47 oligomerization

Wild-type Spa47 and each of the engineered Spa47 mutants were expressed and purified as described above. Spa47 was purified from one-liter cultures and concentrated to 1 mL prior to filtration to remove any insoluble components, and the protein was then evaluated using a GE Superdex 200 16/600 size exclusion column. The column was preequilibrated with 20 mM Tris, 100 mM NaCl, 5 mM DTT, pH 7.9, and operated at 0.5 mL/min. A<sub>280</sub> elution profiles were generated and used to visualize the distribution of monomeric and oligomeric species of the Spa47 proteins. The elution profiles were normalized to the maximum absorbance value for each of the constructs and baseline corrections, and smoothing functions were performed on each of the chromatograms.

### 2.7 | *Shigella* invasion of epithelial cells

Invasion phenotype of *S. flexneri* strains expressing the engineered Spa47 mutants were determined by a gentamicin protection assay as previously described.<sup>22</sup> Sterile 24-well plates were seeded with passaged HeLa cells and grown overnight in DMEM supplemented with 10% fetal calf serum, penicillin, and streptomycin at 100% relative humidity, 37°C, and 5% CO<sub>2</sub>. Evaluated *S. flexneri* strains were streaked onto tryptic soy agar (TSA) plates containing 0.025% Congo Red and grown overnight at 37°C. Small cultures containing appropriate antibiotics were inoculated from the agar plates and grown to an OD<sub>600</sub> of ~0.6 at 37°C and 200 rpm. Equivalent bacterial loads were introduced to the cultured HeLa cells, and the plates were centrifuged at 1000 × g for 5 minutes to synchronize contact between the bacteria and HeLa cells. The inoculated cells were incubated at 37°C for 30 minutes, rinsed to remove extracellular bacteria, and treated with 50 μg/mL gentamicin to selectively kill the *Shigella* that had not successfully invaded the HeLa cells. The HeLa cells were then lysed with 1% agarose in water and overlaid with a LB agar solution. Overnight incubation at 37°C resulted in *Shigella* colony formation from the

previously internalized bacteria, supporting a quantitative comparison of invasion phenotype among the tested *Shigella* strains.

## 2.8 | *Shigella*-induced erythrocyte hemolysis

The effects of the engineered Spa47 mutations on T3SS-mediated hemolysis of red blood cells were determined using a slightly modified version of a previously described method.<sup>23</sup> Briefly, *S. flexneri* expressing wild-type Spa47 or the Spa47 mutants described in this study were grown overnight on TSA-Congo Red plates, and a small number of isolated colonies were used to inoculate 10 mL of tryptic soy broth containing appropriate antibiotics. The cultures were grown to an OD<sub>600</sub> of ~1.0, collected by centrifugation, and gently resuspended in 200  $\mu$ L PBS. Then 50  $\mu$ L of each bacterial mix was combined with  $\sim 5 \times 10^8$  red blood cells in a 96-well microtiter plate and centrifuged at  $2300 \times g$  for 15 minutes to initiate contact between the bacteria and the red blood cells. The plate was then incubated at 37°C for 1 hour and the bacteria/red blood cell mix was resuspended following the addition of 100  $\mu$ L of 4°C PBS. The resuspended mix was centrifuged at  $2300 \times g$  and 10°C for 15 minutes to separate cellular components and the hemoglobin that was released following red blood cell lysis. The levels of released hemoglobin in the supernatant were quantified by measuring absorbance at 545 nm and compared with the released hemoglobin levels resulting from *S. flexneri* expressing wild-type Spa47.

## 2.9 | Quantitation of *S. flexneri* T3SS activation and translocator secretion

The small diazo dye Congo Red effectively induces secretion of translocator proteins through the *Shigella* T3SS by mimicking the natural trigger resulting from host cell membrane interaction.<sup>24</sup> Thus, Congo Red exposure serves as a valuable tool that allows for concerted activation of T3SSs from *Shigella* strains expressing various protein mutants such as the engineered Spa47 mutants used in this study. The Congo Red secretion assay protocol has been described in detail elsewhere.<sup>25</sup> Briefly, a *S. flexneri* strain lacking the gene for Spa47, a strain expressing wild-type Spa47, and strains expressing the engineered Spa47 mutants evaluated in this study were grown overnight on TSA-Congo Red plates and a small number of isolated colonies were used to inoculate 10 mL of tryptic soy broth containing appropriate antibiotics. Cultures were grown at 37°C to an OD<sub>600</sub> of ~1.0 before they were cooled on ice to temporarily slow protein expression and secretion. The cultures were centrifuged and rinsed to separate bacteria from the culture supernatant and any effector proteins that had been secreted up to this point. The cells were then resuspended in sodium phosphate buffer containing 0.28 mg/mL Congo Red and were incubated at 37°C for 1 hour to promote active type three secretion. Cultures were then chilled on ice for 5 minutes to prevent further secretion and the bacteria were separated from the protein-containing supernatant by centrifugation at  $13000 \times g$  for 15 minutes at 4°C. The secreted proteins within the supernatant from each strain were separated using SDS-PAGE, transferred to PVDF membranes by Western blot, and probed using

anti-IpaC rabbit polyclonal antibodies and an Alexa 647 goat anti-rabbit secondary antibody. Secreted IpaC levels were detected and compared using a Bio-Rad ChemiDoc imaging system and the associated Image Lab analysis software. As validated previously,<sup>26</sup> a monoclonal antibody against the cytoplasmic enzyme glyceraldehyde-3-phosphate dehydrogenase (GAPDH) was used as a control in the Western blot to ensure that the proteins observed in the supernatant were secreted from the bacteria and were not the result of cell lysis.

## 2.10 | Spa47 ATP hydrolysis assay

A radioactive  $\alpha$ -<sup>32</sup>P-ATP multiple time point activity assay was used to determine reaction rates for all of the engineered Spa47 mutants in monomeric and oligomeric state. The assay was carried out as described previously.<sup>27</sup> Briefly, the ATPase reactions were initiated at room temperature (20–22°C) by combining protein samples with a prepared ATP solution resulting in a final concentration of 15 mM Tris (pH 7.9), 75 mM NaCl, 10 mM MgCl<sub>2</sub>, 1 mM cold ATP, and 0.5  $\mu$ Ci (~300 nM)  $\alpha$ -<sup>32</sup>P-ATP. Samples were removed from the reaction mixture at defined time points and the reactions rapidly quenched with a final concentration of 250 mM ethylenediaminetetraacetic acid (EDTA). The level of ATP hydrolysis at each time point was quantified by separating the unreacted  $\alpha$ -<sup>32</sup>P-ATP substrate and the  $\alpha$ -<sup>32</sup>P-ADP product by TLC followed by exposure to a phosphor imaging screen and detection of <sup>32</sup>P activity with a Storm PhosphorImager (Molecular Dynamics). The concentration of ADP formed was quantified using ImageQuant software (Molecular Dynamics) and plotted as a function of reaction time to provide a rate of ATP hydrolysis for each enzyme under each condition tested. The final concentration of Spa47 in all reaction conditions was held constant at 0.5  $\mu$ M.

# 3 | RESULTS

## 3.1 | Predicting intermolecular interactions essential for Spa47 oligomerization and activation

An energy minimized model of an activated Spa47 homo-hexamer was generated by aligning the recently solved 2.15 Å Spa47<sup>K165A</sup> structure (PDB ID 5SYP) to each of the protomers of the 2.8 Å hetero-hexameric F1  $\alpha_3\beta_3$  ATP synthase structure (PDB ID 1BMF) using PyMOL,<sup>28</sup> as described previously.<sup>15</sup> The interfaces of adjoining Spa47 protomers within the model were manually searched for interactions that may be involved in supporting Spa47 oligomerization and activation. Two such sites were identified at each interface where residues from one protomer extend across the interface to potentially interact with oppositely charged amino acids from the adjacent protomer (Figure 1), driving and/or stabilizing homo-oligomerization and activation of Spa47. For simplicity, the site containing R271, R272, and E267 that is located near the pore of the hexameric structure will be referred to as "Site 1" (Figure 1A) and the region containing R189, R191, and E287 buried more deeply in the protomer interfaces and located near the active site will be referred to as "Site 2" (Figure 1B). A Clustal Omega sequence alignment of Spa47 and several related T3SS ATPases identifies 100% conservation of all three Site 2 residues

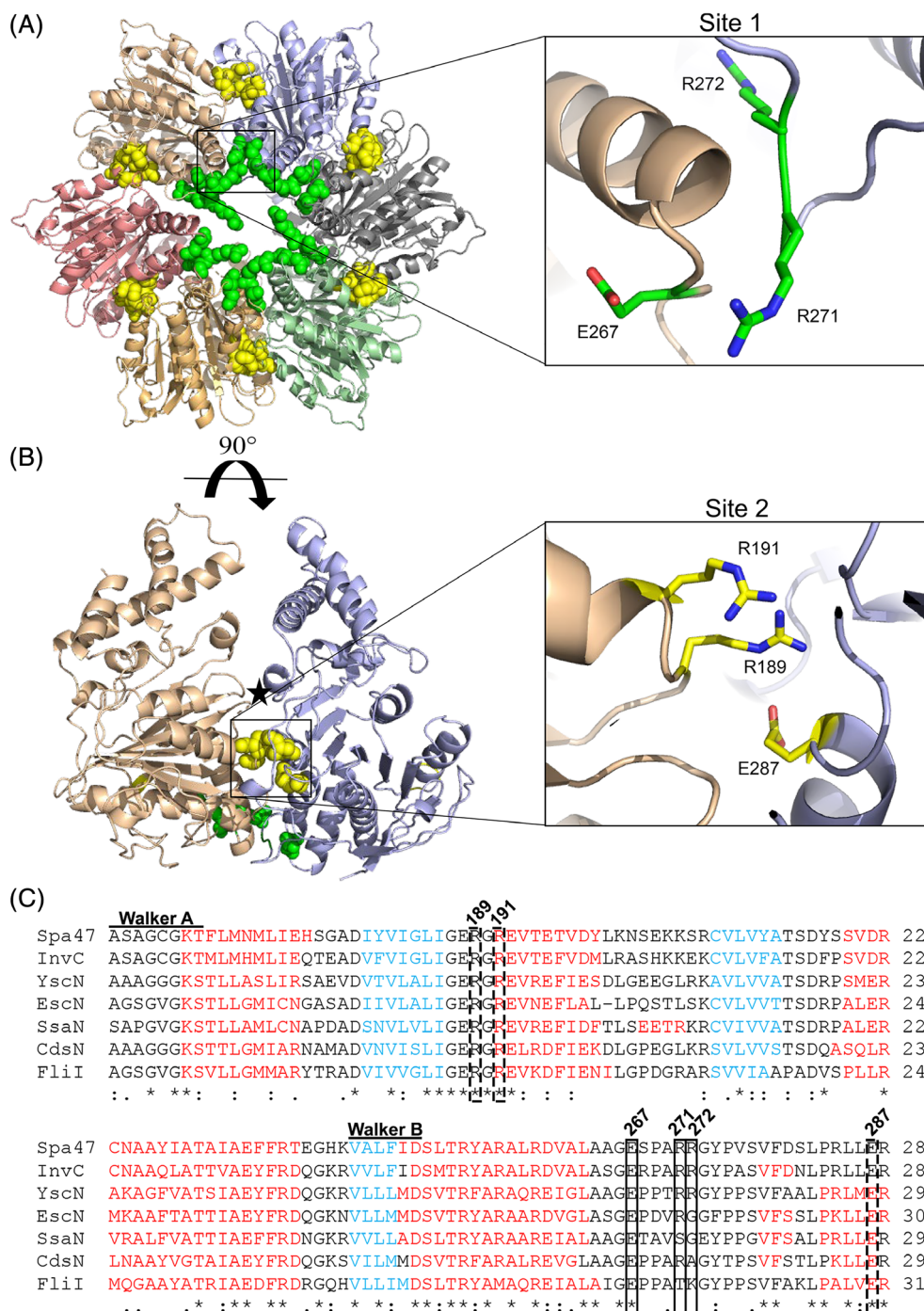


**FIGURE 1** Energy minimized homo-hexameric Spa47 model predicts multiple intermolecular interactions critical for oligomerization and activation. A, Spa47<sup>K165A</sup> (PDB: 5SYP) was modeled as an activated homo-hexamer, based on the hexameric F1 ATP synthase structure (PDB: 1BMF). Each Spa47 monomer subunit is colored independently, while residues in Site 1 are colored in green. The insert provides a closer view of the Site 1 residues with E267 from one protomer and residues R271 and R272 from an adjacent protomer spanning the interface. B, The Spa47 homo-hexameric model is rotated down 90° and all but two of the protomers are removed for clarity. Site 2 residues within the remaining interface are colored in yellow and a black star locates the approximate position of the interfacial active site. The insert shows a closer view of the residues within Site 2 with R189 and R191 from one protomer directed across the interface toward E287 of the adjacent protomer. C, Protein sequence alignment of several T3SS ATPases was performed using the Uniprot multiple sequence alignment tool, Clustal Omega, with single fully conserved residues (\*), conservation between groups with strongly similar properties (:), and weakly similar properties (.) identified. Alpha helix and beta sheet regions, as predicted by the PSIPRED structure prediction server, are color coded red and blue, respectively. Predicted Walker A (P-loop) and Walker B regions are identified, and the Site 1 and Site 2 residues targeted for mutation are identified using solid and dashed boxes, respectively. Uniprot accession numbers used for sequence alignment are Q6XVW8, B5RDL8, P40290, Q7DB71, P74857, F8KX49, and P26465 for Spa47, InvC, YscN, EscN, SsaN, CdsN, and FliI, respectively

(Figure 1C). Site 1, however, shows full conservation of the identified glutamate, but the arginines in Spa47 are both only conserved in the T3SS ATPases InvC from *Salmonella* and YscN from *Yersinia*.

### 3.2 | Engineered Spa47 site 1 and site 2 mutants maintain overall structural integrity

The N-terminal 79 residues were removed from each of the Spa47 proteins to promote crystallization, resulting in 1.85 - 3.00 Å structures for 10 of the 13 engineered Spa47 mutants (Supplementary Table S1 and Supplementary Figure S1). Each of the determined structures closely resemble the wild-type Spa47 structure, with C $\alpha$  RMSD values ranging from 0.31 to 0.45 Å (Figure 2 and Supplementary Figure S1). Thus, the mutations in the ten crystallized constructs do not appear to impact the local or global protein structures, suggesting that changes observed in Spa47 activity, oligomer formation, and *Shigella* virulence phenotype (described below) are due to changes in sidechain characteristics.

### 3.3 | Identified Spa47 residues are critical for proper oligomer formation

Spa47 oligomerization is essential for ATPase activity and *Shigella* virulence, therefore, it was hypothesized that the predicted intermolecular



**FIGURE 2** High-resolution crystal structures of engineered Spa47 oligomerization mutants. Alignment of the previously solved wild-type Spa47 $^{\Delta 1-79}$  structure (gray, PDB ID 5SWJ) to each of the ten Spa47 $^{\Delta 1-79}$  point mutant structures solved in this study (structure coloration is consistent with that used in Supplementary Figure S1) [Color figure can be viewed at [wileyonlinelibrary.com](http://wileyonlinelibrary.com)]

interactions shown in Figure 1 may play important roles in forming and/or stabilizing Spa47 homo-oligomers. Size exclusion chromatography has been a valuable tool in characterizing Spa47 oligomerization and was used here to determine the effect of mutating residues within Site 1 and Site 2 to either alanine or to an opposite charged residue (Figure 3). While mutating E267 within Site 1 to either alanine or arginine has no effect on oligomerization, mutating either R271 or R272 to glutamate significantly reduces the ability for the mutant to form stable oligomers (Figure 3A). Mutating either R271 or R272 to alanine, however, eliminates oligomer formation altogether. Looking at the highly conserved Site 2 shows that mutations to R189 and E287 reduce oligomerization, while all tested mutations targeting R191 abolished Spa47 oligomerization (Figure 3B), confirming that the predicted Site 2 residues all play an important role in Spa47 oligomerization.

### 3.4 | Identified interfacial Spa47 residues influence ATPase activity

We have previously shown that stable Spa47 oligomers exhibit significantly enhanced ATPase activity compared to isolated monomeric Spa47 due to the contribution of active site residues from adjacent protomers upon oligomerization.<sup>15</sup> It seems that transient oligomerization accounts for the low level activity observed for isolated Spa47 monomers, likely utilizing an identical hydrolysis mechanism, but now relying on the formation of a short-lived productive Spa47 $_x$ /ATP complex. The effect of each of the engineered Site 1 and Site 2 mutations on Spa47 ATPase activity was determined using a radioactive  $\alpha$ -<sup>32</sup>P-ATP multiple time point activity assay (Figure 4). The activity results show that the full-length wild-type monomeric and oligomeric Spa47 species behaved as previously reported,<sup>15</sup> hydrolyzing ATP at rates of  $0.20 \pm 0.08$  ( $\mu\text{mol ADP}/\text{min}/\text{mg Spa47}$ ) and  $1.26 \pm 0.22$  ( $\mu\text{mol ADP}/\text{min}/\text{mg Spa47}$ ), respectively. All tested mutations within Site 2 (R189, R191, R189/R191, and E287) abolished ATPase activity regardless of ability to form stable oligomeric species. Interestingly, mutations to the less conserved Site 1 residues, including E267, R271, and R272, had a wider range of effects on the ability of Spa47 to hydrolyze ATP and did not fully eliminate activity of any of the constructs. The alanine and arginine mutations to E267 both maintained the ability to form stable oligomers, however, the mutated oligomers exhibited ATPase activity levels similar to the respective monomers, suggesting that E267 is not essential for stable oligomer formation, but is perhaps necessary for stabilizing the protomer interface to support proper Spa47 ATPase activity. While the R271A and R272A Site 2 mutants both eliminated oligomerization, the monomers continued to function at levels similar to the wild-type monomer ( $0.20 \pm 0.04$  ( $\mu\text{mol ADP}/\text{min}/\text{mg Spa47}$ ) and  $0.33 \pm 0.16$  ( $\mu\text{mol ADP}/\text{min}/\text{mg Spa47}$ ), respectively). The R271E mutant maintained wild-type monomer ATPase levels but attenuated oligomer activity, while the R272E mutation surprisingly maintained wild-type levels for both monomeric and oligomeric species ( $0.31 \pm 0.22$  ( $\mu\text{mol ADP}/\text{min}/\text{mg Spa47}$ ) and  $1.02 \pm 0.28$  ( $\mu\text{mol ADP}/\text{min}/\text{mg Spa47}$ ), respectively).

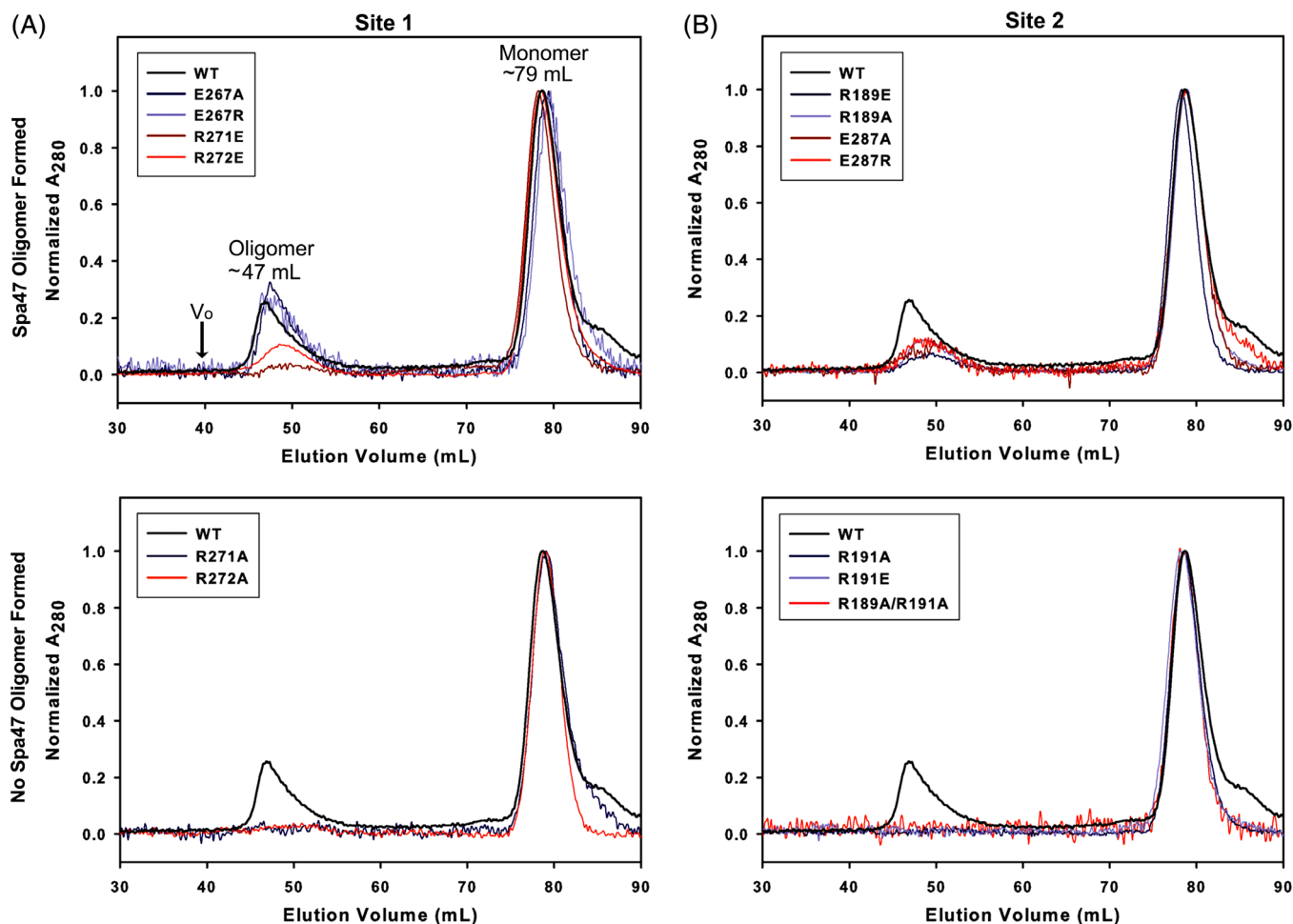


**FIGURE 3** Engineered Spa47 mutations negatively impact homooligomer formation. Size-exclusion chromatography analysis of purified Site 1 (A) and Site 2 (B) Spa47 mutants. The chromatograms from each Spa47 mutant are normalized to the A280 absorbance of the wild-type Spa47 monomer peak eluting at approximately 79 mL. The chromatograms have been further divided into those resulting in detectable levels of Spa47 oligomer formation (top) and those resulting from mutations that eliminated oligomerization (bottom). The void volume ( $V_0$ ) of the column is 39.8 mL and is located with an arrow [Color figure can be viewed at [wileyonlinelibrary.com](http://wileyonlinelibrary.com)]

### 3.5 | Predicted interfacial Spa47 residues support overall *Shigella* virulence phenotype

Insertion of the T3SS translocator tip proteins IpaB and IpaC into the host cell membrane forms the translocon pore and ultimately allows secretion of effector proteins into eukaryotic host cell cytoplasm.<sup>29–32</sup>

Secretion of these effectors into the host cell supports invasion of the infected host cell, escape from the resulting vacuole, and evasion of host immune responses.<sup>4,33,34</sup> To better understand the molecular details of Spa47-mediated *Shigella* virulence, the effect of the engineered Spa47 Site 1 and Site 2 mutations on *Shigella* virulence phenotype were tested using red blood cell hemolysis and gentamicin protection (cellular invasion) assays (Figure 5). With the exception of the R191E and E287A mutations, each of the Site 2 mutations essentially abolished invasion and hemolysis phenotype, consistent with the lack of in vitro ATPase activity observed for these mutants (Figure 4). Surprisingly, even though no ATPase activity was observed in vitro for the Spa47 R191E and E287A mutants, *Shigella* expressing these mutants exhibited moderate invasion and hemolysis levels when compared to *Shigella* expressing

wild-type Spa47, suggesting that additional interactions provided within the T3SA sorting platform must partially mitigate the effects of these mutations in vivo. *Shigella* expressing the Spa47 Site 1 mutations E267A, E267R, and R271A showed at or near wild-type levels of hemolysis ( $116 \pm 12\%$ ,  $108 \pm 8\%$ , and  $91 \pm 19\%$ , respectively) and invasion ( $66 \pm 23\%$ ,  $54 \pm 7\%$ , and  $92 \pm 15\%$ , respectively). Despite forming only monomers in vitro, the R272A mutant supported  $32 \pm 7\%$  invasion and  $18 \pm 6\%$  hemolysis phenotypes, respectively. The R271E and R272E mutants both resulted in severely attenuated levels of both invasion and hemolysis, despite robust in vitro ATPase activity profiles for both monomeric and oligomeric species.

### 3.6 | IpaC secretion profiles provide insight into the effects of engineered Spa47 mutations on T3SS activity and *Shigella* virulence

While the specific mechanism remains unclear and somewhat controversial, Spa47 catalyzed ATP hydrolysis is required for efficient

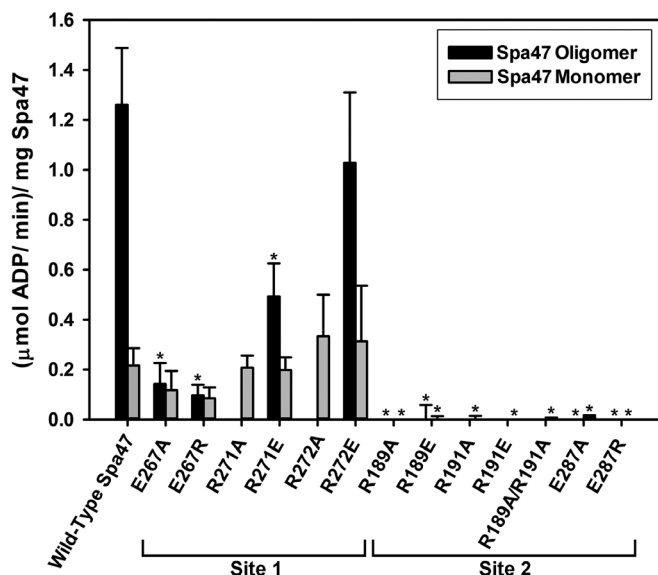


**FIGURE 4** Kinetic analysis of ATP hydrolysis by each of the engineered Spa47 constructs used in this study. Isolated wild-type monomeric and oligomeric Spa47 are both active, with the oligomeric species (black bar) resulting in a significantly enhanced rate of hydrolysis compared to the monomeric form (gray bar). ATP hydrolysis rates were additionally determined for isolated monomeric and oligomeric forms (when available) for all engineered Site 1 and Site 2 Spa47 mutants. Each data set represents the mean  $\pm$  S.D. of three independent kinetic experiments from two independent protein preparations. (\*) Indicates a statistical significance compared to the appropriate oligomer state of wild-type Spa47 (one-way ANOVA followed by a Dunnett's post test,  $P \leq 0.05$ )

protein secretion through the associated needle and tip complex of the *Shigella* T3SA. To determine the effect that the tested Spa47 mutations had on the ability of *Shigella* to actively secrete effector proteins through the T3SA, the levels of the secreted *Shigella* translocator protein IpaC were quantified following Congo Red activation of *Shigella* strains expressing each of the engineered Spa47 Site 1 and Site 2 mutants (Figure 6). Consistent with the hemolysis and invasion results in Figure 5, the Spa47 Site 2 mutants significantly attenuated or eliminated IpaC secretion through the apparatus. The *Shigella* strains expressing Spa47 R191E and Spa47 E287A resulted in low, but detectable secretion levels of IpaC ( $11\% \pm 2\%$  and  $27\% \pm 6\%$ , respectively). Low levels of secreted IpaC were also observed for *Shigella* expressing the Site 1 Spa47 mutants R271E, R272A, and R272E, again tracking well with the hemolysis and invasion phenotypes observed for these strains (Figure 5). Wild-type levels of IpaC secretion were observed for the *Shigella* strain expressing the Spa47 R271A mutant while the E267A and E267R mutations unexpectedly increased IpaC secretion levels to  $233\% \pm 48\%$  and  $146\% \pm 15\%$  of wild-type. These enhanced secretion levels likely support the robust invasion and hemolysis phenotypes of these mutants despite low level ATPase activity observed for the purified mutant oligomers in vitro. With the IpaC secretion profiles in good agreement with the observed *Shigella* virulence phenotypes, it seems clear that the ability of the *Shigella* strains to secrete protein effectors is directly correlated with Spa47 ATPase activity and that

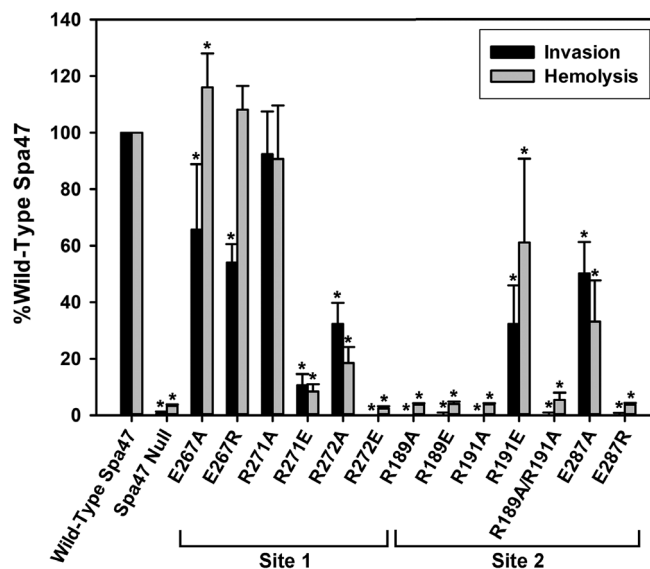


**FIGURE 5** Effect of engineered Spa47 salt bridge mutations on *Shigella* virulence phenotype. The ability of the *Shigella* mutants to invade eukaryotic host cells was measured by a standard gentamicin protection assay. Invasion results (shown in black) are presented as the percentage of invasion by a *S. flexneri* strain expressing wild-type Spa47 and represent at least three independent experimental data sets spanning two biological replicates. The impact of each Spa47 mutant has on *Shigella*'s ability to disrupt phospholipid membranes was examined using a hemolysis assay that quantifies released hemoglobin following incubation of red blood cells with the described *Shigella* mutants. Hemolysis results (shown in gray) are presented as a percentage of the hemoglobin released by the *S. flexneri* strain expressing wild-type Spa47 and result from at least six experiments spanning two biological replicates. Invasion and hemolysis data are both presented as mean values  $\pm$  S.D. (\*) Indicates statistical significance compared to the wild-type Spa47 strain (one-way ANOVA followed by a Dunnett's posttest,  $P \leq 0.05$ )

several of the identified Spa47 Site 1 and Site 2 residues are essential for proper T3SS effector secretion and *Shigella* virulence.

## 4 | DISCUSSION

T3SS are critical virulence factors for a broad class of Gram-negative pathogens, driving significant efforts over the past three decades to uncover their structure, function, activation mechanism(s), and regulatory pathway(s). One mechanistic detail of particular interest is uncovering specifically where the energy comes from that supports protein unfolding and secretion through the narrow apparatus needle. Work primarily focusing on the flagellar T3SS suggests that secretion is driven by proton motive force (PMF) that is coupled to protein secretion through an export gate in the basal body that acts as a proton/protein antiporter.<sup>35-37</sup> While the influence of an electrochemical gradient can certainly not be ruled out, expression of non-catalytic Spa47 mutants eliminates effector secretion and pathogen virulence in *Shigella*, suggesting that at least *Shigella* type three secretion is either independent of PMF and solely reliant on ATP hydrolysis, or more likely that the effects of ATP hydrolysis and

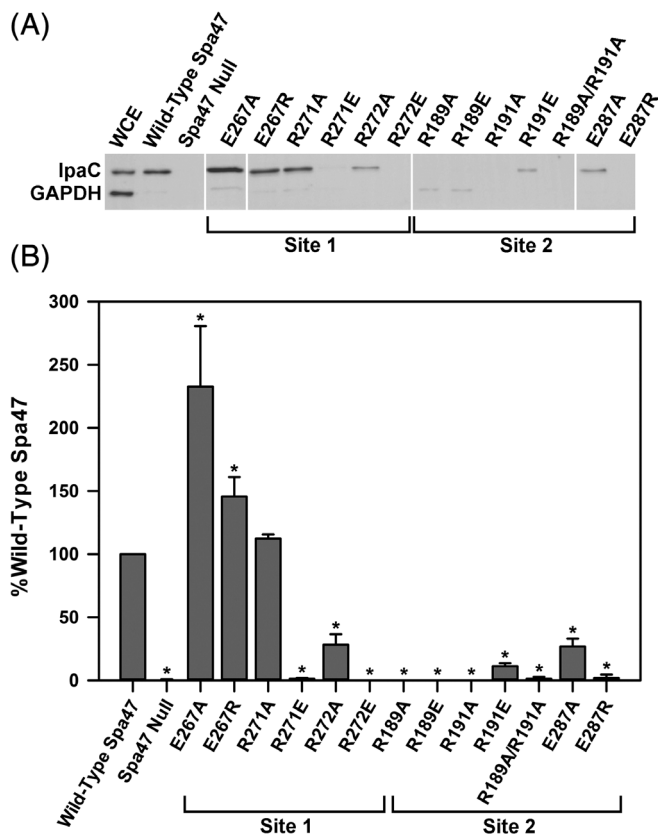


**FIGURE 6** Immunoblot analysis of Congo Red-induced T3SS secretion profiles for engineered Spa47 mutant *Shigella* strains. The levels of IpaC actively secreted following Congo Red induction were compared for *Shigella* strains expressing the Spa47 salt bridge mutants as well as positive and negative controls expressing wild-type Spa47 and a Spa47 null strain, respectively. A, Actively secreted IpaC was detected by Western blot and levels compared using fluorescence densitometry. The cytoplasmic enzyme GAPDH was observed in the whole cell extracts (WCE) but not in the supernatant containing the secreted IpaC protein. B, The secreted IpaC levels are reported relative to a *S. flexneri* strain expressing wild-type Spa47. The reported values represent the means  $\pm$  SD from three independent analyses and two biological replicates. (\*) indicates statistical significance compared to the wild-type Spa47 strain (one-way ANOVA followed by a Dunnett's posttest,  $P \leq 0.05$ )

PMF are synergistic.<sup>15,16</sup> What is clear, however, is that the *Shigella* T3SS relies on Spa47 catalyzed ATP hydrolysis, suggesting that Spa47 may be involved with in vivo activation and regulation of the *Shigella* T3SS and is an attractive target for the development of non-antibiotic small molecule therapeutics.

Like the catalytic hetero-hexameric  $F_1$  and  $V_1$  ATPases, activation of T3SS ATPases requires oligomerization to complete interfacial active sites in the complex. In contrast to the presumably more evolved hetero-hexameric  $F_1$  and  $V_1$  ATPases, however, all enzymatically characterized examples of T3SS ATPases form homo-oligomers.<sup>16,38-43</sup> In vitro studies of T3SS ATPases have identified active complexes ranging from homo-trimers to homo-dodecamers, though cryo-electron imaging of T3SSs from *Shigella* and *Salmonella* both suggest that homo-hexameric T3SS ATPases reside at the base of the apparatus

in vivo.<sup>10,14</sup> Regardless, the importance of oligomerization in activation of T3SS ATPases such as Spa47 underscores the need to better understand not only the specific mechanism of ATP hydrolysis, but also the molecular basis of oligomerization itself.

The work presented here provides insight into Spa47 oligomer formation by identifying two independent sites at the interface of Spa47 protomers that support stable Spa47 oligomer formation, enzymatic activation of isolated Spa47, protein secretion through the T3SA, and overall *Shigella* virulence. Mutating R271 or R272 from Site 1 to alanine or R191 from Site 2 to either alanine or glutamate prevented stable Spa47 oligomerization altogether (Figure 3 and Supplementary Table S2). Interestingly, none of the tested mutations to E267 (Site 1) affected oligomerization while the R271E and R272E reduced, but did not eliminate, Spa47 oligomer formation. All of the tested mutations to Site 2 residues, on the other hand, reduced or eliminated oligomerization, suggesting that while both identified sites play important roles in Spa47 oligomerization, Site 2 has a stronger influence, consistent with the fact that each of the identified Site 2 residues are fully conserved among several well-studied T3SS ATPases (Figure 1C). The influence of the tested Site 1 and Site 2 mutations on enzyme function was demonstrated with an ATPase activity assay, where the mutants targeting Site 1 residues exhibited varying degrees of ATPase activity while ATPase activity of each of the Site 2 mutants was essentially eliminated. In vivo testing of *Shigella* virulence and T3SS-mediated effector secretion also showed the strongest influence by Site 2 mutants, with six of the eight tested Spa47 Site 2 mutants unable to disrupt red blood cell membranes or infect cultured eukaryotic cells. Not surprisingly, these virulence phenotypes correlate quite well with T3SS effector protein (IpaC) secretion levels, showing that protein secretion is linked to Spa47 catalyzed ATP hydrolysis and that *Shigella* virulence is driven by protein secretion through the T3SA. Surprisingly, despite being ATPase inactive in vitro, the Site 2 Spa47 R191E and E287A mutants exhibited modest, yet robust, invasion, hemolysis, and effector secretion capabilities, suggesting that additional interactions within the T3SA can overcome the effects of these mutations and support Spa47 oligomerization/activation in vivo. While the data reported in this study clearly show that the identified Spa47 interfaces are involved in supporting oligomerization and ATPase activity, specific molecular insight into the intermolecular interactions involving the Site 1 and Site 2 residues was unavailable until Majewski and colleagues published a 3.3 Å cryo-EM structure of the *E. coli* homo-hexameric T3SS ATPase EscN during the preparation of this manuscript.<sup>44</sup>

The cryo-EM structure of EscN is currently the only high-resolution structure available for an activated homo-hexameric T3SS ATPase, providing valuable insight into the conformational changes and intermolecular interactions responsible for ATP hydrolysis and a structural rationale for the effects observed in the Spa47 mutants engineered in this study. Specifically, the homo-hexameric EscN structure includes the central stalk protein EscO as well as the transition state analog  $Mg^{2+}$  ADP-AIF<sub>3</sub> in four of the six EscN protomer interfaces, displaying conformational changes reminiscent of those supporting ATP synthesis/hydrolysis in rotary

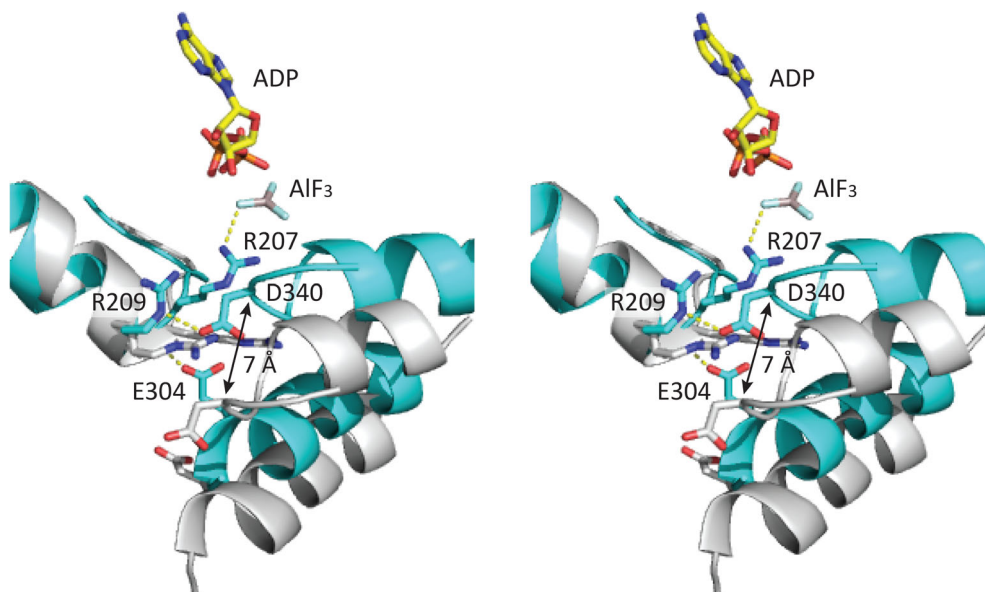


**FIGURE 7** Conserved EscN Site 2 residues provide critical noncovalent intermolecular interactions and insight into Spa47 oligomerization and activation. A stereo image of the aligned EscN active sites and Site 2 residues from an apo (gray) and nucleotide-bound (cyan) protomer interface was generated from the published cryo-EM EscN homo-hexameric structure (PDB ID 6NJP).<sup>44</sup> Significant structural rearrangement within the nucleotide-bound interface (cyan) favorably positions the conserved Site 2 residues for intermolecular hydrogen bonding across the protomer interface (dashed lines) and positions arginine 207 to stabilize the substrate and support catalysis. All of the residues involved in this EscN intermolecular hydrogen bonding network are conserved in Spa47 and are likely responsible for the altered Spa47 oligomerization characteristics and *Shigella* phenotypes observed for Spa47 Site 2 mutants [Color figure can be viewed at [wileyonlinelibrary.com](http://wileyonlinelibrary.com)]

F- and V-type hetero-hexameric ATPases.<sup>44</sup> Superposition of nucleotide-free and nucleotide bound active sites reveals significant conformational rearrangements at the protomer interface (Figure 7, stereo image). The transition from nucleotide-free to nucleotide-bound states involves a shift of up to 7 Å between individual monomers at the interface. The shift engages an intermolecular hydrogen bonding network that includes Site 2 residues. Two of these hydrogen bonds are observed between the EscN R209 (R191 in Spa47) and D340 (D324 in Spa47) sidechains, and between the sidechain of E304 (E287 in Spa47) and the backbone of G208 (G190 in Spa47). As a consequence, R207 (R189 in Spa47) is positioned to coordinate the gamma phosphate of ATP, presumably facilitating phosphate hydrolysis. This is in good agreement with the results presented here as all of the tested mutations to Spa47 R189 lacked ATPase activity and exhibited avirulent phenotypes while *Shigella* strains expressing mutations to the conserved R191 and E287 residues ranged from avirulent to modestly virulent depending on the identity of the mutation.

Together, the findings presented here have identified two independent sites that reside at the interface between Spa47 protomers to support oligomerization and activation of Spa47, protein secretion through the T3SA, and overall *Shigella* virulence. Insights from a recently solved EscN homo-hexameric cryo-EM structure suggest that the Site 2 residues directly influence ATP hydrolysis in addition to supporting oligomerization, while the Site 1 residues are located much further from the active site and are likely not directly involved in catalysis, but do contribute intermolecular hydrogen bonds that support oligomer formation and stabilize local structural elements. Fully

understanding the influences of the identified residues on Spa47 activity and type three secretion will likely require a series of biochemical and biophysical studies spanning T3SS ATPases from other pathogens as well as structural and perhaps single molecule fluorescence studies. Predicting and characterizing the influence of the tested mutations in this study, however, begins to paint a picture of how Spa47 is activated and uncovers much needed targets for non-antibiotic small molecule therapeutics that should inhibit Spa47 ATPase activity and may be effective in targeting the conserved sites of additional T3SS ATPases such as EscN.

## ACKNOWLEDGMENTS

This work was supported in part by a National Institutes of Health Grant 1R15AI124108-01A1 and R. Gaurth Hansen endowment funds to N. E. D. and an NSF MRI (1530862) to S. J. H. J. D. received support from a Utah State University Undergraduate Research and Creative Opportunity Grant. Use of the Stanford Synchrotron Radiation Lightsource, SLAC National Accelerator Laboratory is supported by the U.S. Department of Energy, Office of Science, Office of Basic Energy Sciences under Contract No. DE-AC02-76SF00515. The SSRL Structural Molecular Biology Program is supported by the DOE Office of Biological and Environmental Research, and by the National Institutes of Health, National Institute of General Medical Sciences (including P41GM103393). The contents of this publication are solely the responsibility of the authors and do not necessarily represent the official views of NIGMS, NIAID, NIH, or NSF.

## CONFLICT OF INTERESTS

The authors declare no potential conflict of interest.

## ORCID

Hannah J. Demler  <https://orcid.org/0000-0003-3508-9554>

Heather B. Case  <https://orcid.org/0000-0002-5323-4973>

Yalemi Morales  <https://orcid.org/0000-0001-9697-099X>

Abram R. Bernard  <https://orcid.org/0000-0001-7681-7728>

Sean J. Johnson  <https://orcid.org/0000-0001-7992-2494>

Nicholas E. Dickenson  <https://orcid.org/0000-0003-1572-6077>

## REFERENCES

- DuPont HL, Levine MM, Hornick RB, Formal SB. Inoculum size in shigellosis and implications for expected mode of transmission. *J Infect Dis.* 1989;159:1126-1128.
- Kotloff KL, Nataro JP, Blackwelder WC, et al. Burden and aetiology of diarrhoeal disease in infants and young children in developing countries (the global enteric multicenter study, GEMS): a prospective, case-control study. *Lancet.* 2013;382:209-222.
- Dutta S, Ghosh A, Ghosh K, et al. Newly emerged multiple-antibiotic-resistant *Shigella dysenteriae* type 1 strains in and around Kolkata, India, are clonal. *J Clin Microbiol.* 2003;41:5833-5834.
- Schroeder GN, Hilbi H. Molecular pathogenesis of *Shigella* spp.: controlling host cell signaling, invasion, and death by type III secretion. *Clin Microbiol Rev.* 2008;21:134-156.
- Deng W, Marshall NC, Rowland JL, et al. Assembly, structure, function and regulation of type III secretion systems. *Nat Rev Microbiol.* 2017;15:323-337.
- Portaliou AG, Tsois KC, Loos MS, Zorzini V, Economou A. Type III secretion: building and operating a remarkable nanomachine. *Trends Biochem Sci.* 2016;41:175-189.
- Galan JE, Lara-Tejero M, Marlovits TC, Wagner S. Bacterial type III secretion systems: specialized nanomachines for protein delivery into target cells. *Annu Rev Microbiol.* 2014;68:415-438.
- Wagner S, Grin I, Malmshaimer S, Singh N, Torres-Vargas CE, Westerhausen S. Bacterial type III secretion systems: a complex device for the delivery of bacterial effector proteins into eukaryotic host cells. *FEMS Microbiol Lett.* 2018;365. <https://www.ncbi.nlm.nih.gov/pubmed/30107569>.
- Kubori T, Matsushima Y, Nakamura D, et al. Supramolecular structure of the salmonella typhimurium type III protein secretion system. *Science.* 1998;280:602-605.
- Hu B, Morado DR, Margolin W, et al. Visualization of the type III secretion sorting platform of *Shigella flexneri*. *Proc Natl Acad Sci U S A.* 2015;112:1047-1052.
- Epler CR, Dickenson NE, Bullitt E, Picking WL. Ultrastructural analysis of IpaD at the tip of the nascent MxiH type III secretion apparatus of *Shigella flexneri*. *J Mol Biol.* 2012;420:29-39.
- Hu J, Worrall LJ, Hong C, et al. Cryo-EM analysis of the T3S injectisome reveals the structure of the needle and open secretin. *Nat Commun.* 2018;9:3840.
- Park D, Lara-Tejero M, Waxham MN, et al. Visualization of the type III secretion mediated salmonella-host cell interface using cryo-electron tomography. *Elife.* 2018;7:e39514.
- Hu B, Lara-Tejero M, Kong Q, Galan JE, Liu J. In situ molecular architecture of the salmonella type III secretion machine. *Cell.* 2017;168(1065-1074):e1010.
- Burgess JL, Burgess RA, Morales Y, Bouvang JM, Johnson SJ, Dickenson NE. Structural and biochemical characterization of Spa47 provides mechanistic insight into type III secretion system ATPase activation and *Shigella* virulence regulation. *J Biol Chem.* 2016;291:25837-25852.
- Burgess JL, Jones HB, Kumar P, et al. Spa47 is an oligomerization-activated type three secretion system (T3SS) ATPase from *Shigella flexneri*. *Protein Sci.* 2016;25:1037-1048.
- Case HB, Mattock DS, Dickenson NE. Shutting down *Shigella* secretion: characterizing small molecule type three secretion system ATPase inhibitors. *Biochemistry.* 2018;57:6906-6916.
- Formal SB, Dammin GJ, Labrec EH, Schneider H. Experimental *Shigella* infections: characteristics of a fatal infection produced in Guinea pigs. *J Bacteriol.* 1958;75:604-610.
- Jouihri N, Sory MP, Page AL, Gounon P, Parsot C, Allaoui A. MxiK and MxiN interact with the Spa47 ATPase and are required for transit of the needle components MxiH and MxiI, but not of Ipa proteins, through the type III secretion apparatus of *Shigella flexneri*. *Mol Microbiol.* 2003;49:755-767.
- Otwinowski Z, Minor W. Processing of X-ray diffraction data collected in oscillation mode. *Method Enzymol.* 1997;276:307-326.
- Adams PD, Afonine PV, Bunkoczi G, et al. PHENIX: a comprehensive python-based system for macromolecular structure solution. *Acta Crystallogr D.* 2010;66:213-221.
- Niesel DW, Chambers CE, Stockman SL. Quantitation of HeLa cell monolayer invasion by *Shigella* and salmonella species. *J Clin Microbiol.* 1985;22:897-902.
- Sansonetti PJ, Ryter A, Clerc P, Maurelli AT, Mounier J. Multiplication of *Shigella flexneri* within HeLa cells: lysis of the phagocytic vacuole and plasmid-mediated contact hemolysis. *Infect Immun.* 1986;51:461-469.
- Menard R, Sansonetti PJ, Parsot C. Nonpolar mutagenesis of the ipa genes defines IpaB, IpaC, and IpaD as effectors of *Shigella flexneri* entry into epithelial cells. *J Bacteriol.* 1993;175:5899-5906.
- Parsot C, Menard R, Gounon P, Sansonetti PJ. Enhanced secretion through the *Shigella flexneri* mxi-Spa translocon leads to assembly of extracellular proteins into macromolecular structures. *Mol Microbiol.* 1995;16:291-300.
- Bernard AR, Jessop TC, Kumar P, Dickenson NE. Deoxycholate-enhanced *Shigella* virulence is regulated by a rare pi-helix in the type three secretion system tip protein IpaD. *Biochemistry.* 2017;56:6503-6514.
- Case HB, Dickenson NE. Kinetic characterization of the *Shigella* type three secretion system ATPase Spa47 using alpha-(32)P ATP. *Bio Protoc.* 2018;8:3074.
- The PyMOL Molecular Graphics System, version 1.8, Schrödinger, LLC.
- Blocker A, Gounon P, Larquet E, et al. The tripartite type III secretin of *Shigella flexneri* inserts IpaB and IpaC into host membranes. *J Cell Biol.* 1999;147:683-693.
- Dickenson NE, Picking WD. Forster resonance energy transfer (FRET) as a tool for dissecting the molecular mechanisms for maturation of the *Shigella* type III secretion needle tip complex. *Int J Mol Sci.* 2012;13:15137-15161.
- Dickenson NE, Arizmendi O, Patil MK, et al. N-terminus of IpaB provides a potential anchor to the *Shigella* type III secretion system tip complex protein IpaD. *Biochemistry.* 2013;52:8790-8799.
- Adam PR, Dickenson NE, Greenwood JC 2nd, Picking WL, Picking WD. Influence of oligomerization state on the structural properties of invasion plasmid antigen B from *Shigella flexneri* in the presence and absence of phospholipid membranes. *Proteins.* 2014;82:3013-3022.
- Killackey SA, Sorbara MT, Girardin SE. Cellular aspects of *Shigella* pathogenesis: focus on the manipulation of host cell processes. *Front Cell Infect Microbiol.* 2016;6:38.
- Picking WL, Picking WD. The many faces of IpaB. *Front Cell Infect Microbiol.* 2016;6:12.
- Erhardt M, Mertens ME, Fabiani FD, Hughes KT. ATPase-independent type-III protein secretion in *Salmonella enterica*. *PLoS Genet.* 2014;10:e1004800.

36. Wilharm G, Lehmann V, Krauss K, et al. Yersinia enterocolitica type III secretion depends on the proton motive force but not on the flagellar motor components MotA and MotB. *Infect Immun*. 2004;72:4004-4009.
37. Minamino T, Morimoto YV, Hara N, Aldridge PD, Namba K. The bacterial flagellar type III export gate complex is a dual fuel engine that can use both H<sup>+</sup> and Na<sup>+</sup> for flagellar protein export. *PLoS Pathog*. 2016;12:e1005495.
38. Minamino T, Kazetani K, Tahara A, et al. Oligomerization of the bacterial flagellar ATPase FliI is controlled by its extreme N-terminal region. *J Mol Biol*. 2006;360:510-519.
39. Stone CB, Johnson DL, Bulir DC, Gilchrist JD, Mahony JB. Characterization of the putative type III secretion ATPase CdsN (Cpn0707) of chlamydomphila pneumoniae. *J Bacteriol*. 2008;190:6580-6588.
40. Andrade A, Pardo JP, Espinosa N, Perez-Hernandez G, Gonzalez-Pedrajo B. Enzymatic characterization of the enteropathogenic *Escherichia coli* type III secretion ATPase EscN. *Arch Biochem Biophys*. 2007;468:121-127.
41. Muller SA, Pozidis C, Stone R, et al. Double hexameric ring assembly of the type III protein translocase ATPase HrcN. *Mol Microbiol*. 2006;61:119-125.
42. Claret L, Calder SR, Higgins M, Hughes C. Oligomerization and activation of the FliI ATPase central to bacterial flagellum assembly. *Mol Microbiol*. 2003;48:1349-1355.
43. Akeda Y, Galan JE. Genetic analysis of the *Salmonella enterica* type III secretion-associated ATPase InvC defines discrete functional domains. *J Bacteriol*. 2004;186:2402-2412.
44. Majewski DD, Worrall LJ, Hong C, et al. Cryo-EM structure of the homohexameric T3SS ATPase-central stalk complex reveals rotary ATPase-like asymmetry. *Nat Commun*. 2019;10:626.

## SUPPORTING INFORMATION

Additional supporting information may be found online in the Supporting Information section at the end of this article.

**How to cite this article:** Demler HJ, Case HB, Morales Y, Bernard AR, Johnson SJ, Dickenson NE. Interfacial amino acids support Spa47 oligomerization and *shigella* type three secretion system activation. *Proteins*. 2019;87:931-942.  
<https://doi.org/10.1002/prot.25754>